Geophysical Journal International

Geophys. J. Int. (2015) **203,** 416–427
GJI Geodynamics and tectonics

doi: 10.1093/gji/ggv277

High-resolution Neogene and Quaternary estimates of Nubia-Eurasia-North America Plate motion

C. DeMets,[1] G. Iaffaldano[2,*] and S. Merkouriev[3,4]

[1]*Department of Geoscience, University of Wisconsin-Madison, Madison, WI* 53706, *USA. E-mail: chuck@geology.wisc.edu*
[2]*Research School of Earth Sciences, Australian National University, Acton, ACT* 2601, *Australia*
[3]*Pushkov Institute of Terrestrial Magnetism, Russian Academy of Sciences, St Petersburg* 199034, *Russia*
[4]*Saint Petersburg State University, Institute of Earth Sciences Universitetskaya nab.,* 7-9, *St. Petersburg* 199034, *Russia*

Accepted 2015 June 24. Received 2015 June 22; in original form 2015 March 27

SUMMARY

Reconstructions of the history of convergence between the Nubia and Eurasia plates constitute an important part of a broader framework for understanding deformation in the Mediterranean region and the closing of the Mediterranean Basin. Herein, we combine high-resolution reconstructions of Eurasia-North America and Nubia-North America Plate motions to determine rotations that describe Nubia-Eurasia Plate motion at ∼1 Myr intervals for the past 20 Myr. We apply trans-dimensional hierarchical Bayesian inference to the Eurasia-North America and Nubia-North America rotation sequences in order to reduce noise in the newly estimated Nubia-Eurasia rotations. The noise-reduced rotation sequences for the Eurasia-North America and Nubia-North America Plate pairs describe remarkably similar kinematic histories since 20 Ma, consisting of relatively steady seafloor spreading from 20 to 8 Ma, ∼20 per cent opening-rate slowdowns at 8–6.5 Ma, and steady plate motion from ∼7 Ma to the present. Our newly estimated Nubia-Eurasia rotations predict that convergence across the central Mediterranean Sea slowed by ∼50 per cent and rotated anticlockwise after ∼25 Ma until 13 Ma. Motion since 13 Ma has remained relatively steady. An absence of evidence for a significant change in motion immediately before or during the Messinian Salinity Crisis at 6.3–5.6 Ma argues against a change in plate motion as its causative factor. The detachment of the Arabian Peninsula from Africa at 30–24 Ma may have triggered the convergence rate slowdown before 13 Ma; however, published reconstructions of Nubia-Eurasia motion for times before 20 Ma are too widely spaced to determine with confidence whether the two are correlated. A significant discrepancy between our new estimates of Nubia-Eurasia motion during the past few Myr and geodetic estimates calls for further investigation.

Key words: Plate motions; Continental margins: convergent; Neotectonics.

1 INTRODUCTION

Convergence between Africa and Eurasia has been the principal cause of deformation in the Mediterranean region during the Cenozoic, including the Alpine orogeny, backarc extension that dominates much of the Mediterranean's present tectonics (Jolivet & Faccenna 2000; Jolivet *et al.* 2006), and the progressive closing of the Mediterranean Sea, which set the stage for the Messinian Salinity Crisis and its associated climatic effects (Ivanovic *et al.* 2014). Well-determined reconstructions of Africa-Eurasia Plate motion constitute an important part of the framework for better understanding these deformation events as well as the geological and geodynamic evolution of much of the Mediterranean region (e.g. Jolivet & Faccenna 2000; ArRajehi *et al.* 2010; Reilinger & McClusky 2011; Vissers & Meijer 2012). Numerous authors have reconstructed the motion of Africa relative to Eurasia from finite rotations that reconstruct Arctic and Atlantic basin magnetic anomalies and fracture zones that record Africa-North America and Eurasia-North America Plate motion (e.g. Dewey *et al.* 1989; Mazzoli & Helman 1994; Rosenbaum *et al.* 2002; McQuarrie *et al.* 2003; Vissers & Meijer 2012). These reconstructions indicate that roughly N–S directed convergence between Africa and Eurasia commenced between 120 and 83 Ma (Rosenbaum *et al.* 2002). Convergence since then has been slower than ∼20 km Myr^{-1} across the Mediterranean Sea and has included a period of slow or possibly no convergence from 67 to 55 Ma, a possible convergence speedup from ∼50 to 35 Ma, and a slowdown after ∼35 Ma to present rates of only several km Myr^{-1} (Rosenbaum *et al.* 2002).

To date, reconstructions of Nubia-Eurasia plate motion during the Quaternary and Neogene, the period considered in this study,

*Now at: Department of Geosciences and Natural Resource Management, University of Copenhagen, Denmark.

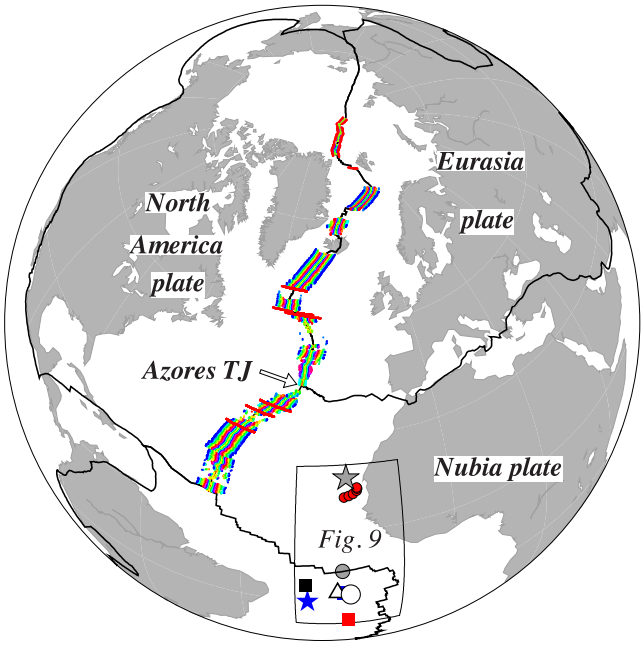

Figure 1. Locations of magnetic reversal, transform fault and fracture zone data (coloured circles) from Merkouriev & DeMets (2014a,b) that are used to estimate Nubia-Eurasia rotations in this study. The observations consist of 13 244 and 12 866 magnetic reversal, fracture zone and transform fault crossings from the Eurasia-North America and Nubia-North America Plate boundaries, respectively. Crossings of 21 magnetic reversals that range from C1n (0.78 Ma) to the old edge of C6n (19.72 Ma) constrain the rotations. Symbols in the inset rectangle show Nubia-Eurasia poles that are discussed in the text and displayed in Fig. 9. 'TJ' is triple junction.

have been limited to Anomaly 2A (∼3 Ma), Anomaly 5 (∼10 Ma) and Anomaly 6 (∼20 Ma). All three of these magnetic anomalies are well surveyed and easily identified in most of the northern Atlantic and Arctic basins, making them well suited for estimating reliable reconstructions. Unfortunately, these reconstructions are too widely spaced in time to permit strong tests of whether and when plate motion has changed during the past 20 Myr and if so, whether any changes in motion preceded or coincided with geologically significant events such as the Mediterranean Salinity Crisis at 6.3–5.6 Ma (Rouchy & Caruso 2006).

Herein, we use high-resolution Quaternary and Neogene rotation sequences for the Eurasia-North America and Nubia-North America Plate pairs (Merkouriev & DeMets 2014a,b) to estimate the first high-resolution reconstructions of Nubia-Eurasia Plate motion during the Quaternary and much of the Neogene. Derived from more than 20 000 magnetic reversal, transform fault, and fracture zone crossings from seafloor spreading centres in the Arctic basin and the Mid-Atlantic Ridge north of 15°N (Fig. 1), the new rotations are constrained by many more kinematic observations than in previous studies and reconstruct Nubia-Eurasia-North America Plate motions at ∼1 Myr intervals since 20 Ma, much better than in previous studies.

An important focus of our analysis is to improve the signal-to-noise ratio in the Eurasia-North America and Nubia-North America rotations from which we estimate the Nubia-Eurasia rotations. Nubia-Eurasia motion has ranged from only 2 to 10 mm yr^{-1} since 20 Ma along most of the plate boundary (DeMets *et al.* 2010; Reilinger & McClusky 2011). Net movement of as little as 2 km between the two plates has thus occurred during the ∼1 Myr intervals that separate our closely spaced rotations. Errors of only ±1 km in reconstructing the relative positions of the two plates can thus introduce a ∼50 per cent error into rates that average motion over only a 1 Myr long period.

As a means of reducing the noise that propagates into the Nubia-Eurasia rotations from the Eurasia-North America and Nubia-North America rotations, we use trans-dimensional, hierarchical Bayesian inference, an effective method for reducing the impact of noise on sequences of finite rotations and their associated stage Euler vectors (Iaffaldano *et al.* 2012; Iaffaldano *et al.* 2014). Specifically, we apply Bayesian inference to the Quaternary/Neogene rotation sequences for the Eurasia-North America and Nubia-North America plate pairs to reduce the noise in each rotation sequence and hence the noise that propagates into Nubia-Eurasia rotation estimates. This reduces the probability that the new, closely spaced rotations will predict implausibly rapid and large variations in the torques that have acted on the Nubia, Eurasia, and North America plates during the past 20 Myr (e.g. Iaffaldano *et al.* 2012).

2 DATA USED TO DERIVE FINITE ROTATIONS

The Eurasia-North America rotation sequence that we use as one starting point for our analysis was derived by Merkouriev & DeMets (2014a) from an inversion of more than 11 000 crossings of 21 magnetic polarity reversals younger than and including C6no (19.72 Ma), as well as several thousand crossings of the Charlie Gibbs, Bight and Spitsbergen transform faults and fracture zones (Fig. 1). All of these data are from the Arctic basin spreading centres, the Reykjanes Ridge, or the Mid-Atlantic Ridge south to the Azores Triple Junction at ∼39°N. All ∼11 000 of the original data that were used to estimate these rotations are provided in the Supporting Information documents.

The Nubia-North America rotations that are the other starting point for our analysis were derived by Merkouriev & DeMets (2014b) from nearly 11 000 crossings of the same 21 magnetic reversals and several thousand more crossings of the Atlantis, Hayes, and Oceanographer transform faults and fracture zones (Fig. 1). These data are from the Nubia-North America segment of the Mid-Atlantic Ridge, which extends from 15°N to 38°N. The Nubia-North America rotations reconstruct the same 21 magnetic reversals as do the Eurasia-North America rotations. The two can thus be combined without any interpolation to find Nubia-Eurasia rotations (and their covariances). All of the data that were used to determine these rotations are provided in the supplemental documents.

All 20 000+ magnetic reversal identifications that are used in the two studies cited above were determined from original airborne and shipboard magnetic data. Transform faults and fracture zones were digitized from a combination of multi-beam, single-beam, and satellite-derived bathymetry from the Marine Geoscience Data System (www.marine-geo.org and Carbotte *et al.* 2004). Readers are referred to Merkouriev & DeMets (2014a,b) for further information.

3 IMPACT AND REDUCTION OF FINITE-ROTATION NOISE

Noise propagates into estimates of finite plate rotations from a multiplicity of random and systematic sources that include but are not limited to navigational errors in seafloor and fracture zone surveys, variability in the linearity of magnetic reversals, outward displacement and/or misidentifications of magnetic reversals, and difficulties in using oceanic fracture zones to constrain palaeo-slip

directions between plates. Differentiating a time sequence of finite rotations in order to estimate stage rotations further amplifies the noise, possibly complicating attempts to identify changes in plate motion. Noisy stage rotations may also predict rapid variations in plate motion that are geodynamically implausible in light of the variations in plate-driving torques that would be required to drive such kinematic changes (Iaffaldano *et al.* 2013).

To mitigate these problems, we use 'REDBACK' software, a recently developed, open-source software that applies trans-dimensional, hierarchical Bayesian inference to time sequences of finite rotations in order to reduce noise (Iaffaldano *et al.* 2014). The way that Bayesian inference achieves this is best explained through a comparison to the method by which the most representative value of a physical observable is estimated. Given a statistically significant number of measurements of an observable, its most representative value is neither any particular measurement nor the most certain measurement, but is instead the weighted average, which takes into account the uncertainty of each measurement. Similarly, REDBACK applies Monte Carlo algorithms to a starting sequence of finite rotations to generate numerous candidate models of finite rotation sequences, none of which is considered more probable than any other candidate model at the start of the process. Based on a comparison of each candidate model to the starting rotation sequence, each candidate model is assigned a probability of being a faithful realization of the truth given the noisy rotations that are available. The probability for each candidate model is proportional to its distance from the noisy, starting rotations.

By generating millions of models, one samples the posterior distribution of probability—that is, the probability associated with a given sequence of rotations after having compared it to the available rotations. Markov Chain methods make the sampling computationally efficient on personal computers. As with repeated measurements, the most representative model is defined as the weighted average of the models according to the sampled posterior probability. Iaffaldano *et al.* (2014) demonstrates that the above procedure correctly identifies a finite rotation sequence that is closer to a noise-free sequence of synthetic starting rotations than to the same sequence of rotations perturbed by realistic levels of rotation noise. We refer readers to Iaffaldano *et al.* (2014) for more details.

4 RESULTS

Below, we describe and compare the newly estimated, noise-reduced rotations for the Eurasia-North America and Nubia-North America Plate pairs to the best-fitting rotations from which they were estimated. We then derive and describe Nubia-Eurasia finite rotations from the Eurasia-North America and Nubia-North America rotations and use the newly estimated finite rotations and their corresponding stage angular velocities to describe how Nubia-Eurasia Plate motion has evolved during the past 20 Myr.

4.1 Eurasia-North America kinematics since 20 Ma

4.1.1 Best-fitting finite rotations

The Eurasia-North America finite opening poles that best reconstruct the numerous magnetic reversal and fracture zone crossings from the northern Mid-Atlantic Ridge and Arctic basin (from table 2 of Merkouriev & DeMets 2014a) are clustered between 60.5°N and 71°N (Fig. 2a) and migrate generally southward through time. Occasional erratic changes in the path described by the best-fitting

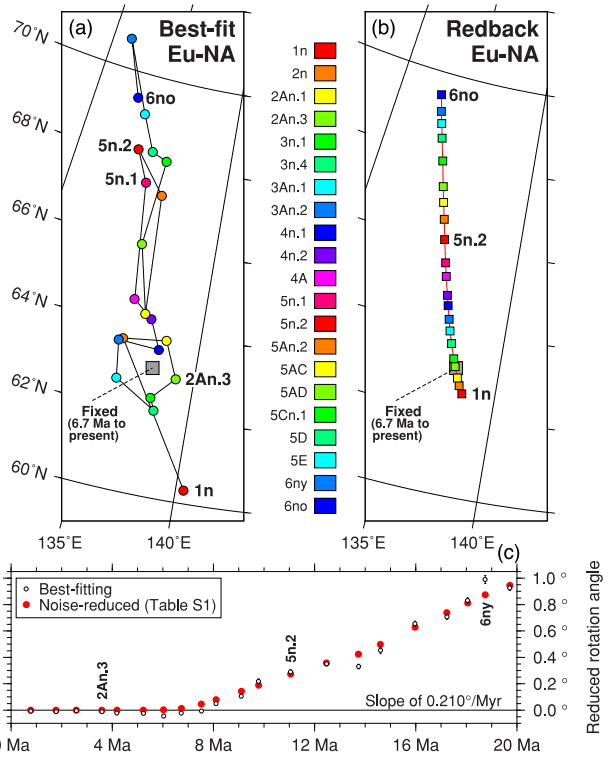

Figure 2. Comparison of Eurasia-North America finite rotation poles and angles before and after noise reduction. (a) Best-fitting finite rotation poles from table 2 of Merkouriev & DeMets (2014a). (b) Finite rotation poles from REDBACK noise-reduction analysis (Supporting Information Table 1). The grey square denotes the location of the Eurasia-North America pole from Merkouriev & DeMets (2014a) for a model that enforces a stationary pole and constant rate of angular rotation since 6.7 Ma. (c) Best-fitting and noise-reduced opening angles reduced by a slope of 0.210° Myr^{-1}.

poles reflects noise propagated from the underlying kinematic observations rather than real changes in motion. Significant noise is also apparent in the best-fitting opening angles (Fig. 2c), particularly for reversals older than ∼13 Ma due to the smaller number of data from which some of those rotations are determined and the difficulty in identifying the precise locations of some of the shorter-duration, lower-amplitude magnetic anomalies that are associated with reversals C5AC through C5Cn.3 (13.7–16.7 Ma).

4.1.2 Noise-reduced rotations and fits

The finite rotations that we derived from a REDBACK analysis of the original, best-fitting rotations (Supporting Information Table 1) migrate smoothly southward with time (Fig. 2b) and are more clustered than are the noisier best-fitting poles. The REDBACK rotation angles also change less erratically than do the best-fitting angles (Fig. 2c). Bayesian inference thus successfully reduces noise in the plate kinematic evolution that is otherwise implied by the best-fitting rotations.

In order to determine the fitting penalty that is introduced by Bayesian inference, we reconstructed all ∼11 000 of the original Eurasia-North America magnetic reversal and fracture zone crossings with the noise-reduced and best-fitting rotations and compared their respective fits. Flow lines reconstructed with the new REDBACK stage rotations (Supporting Information Table 2) for both strands of the well-mapped Charlie Gibbs Fracture Zone (black lines in the upper panel of Fig. 3) differ by less than a few hundred

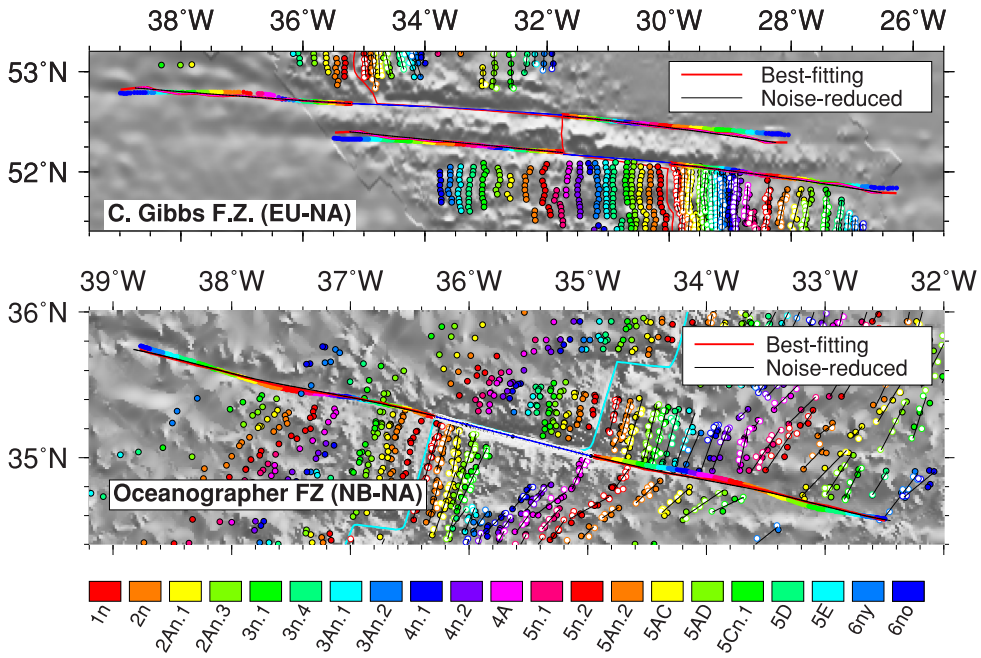

Figure 3. Best-fitting (red) and noise-reduced (black) flow lines predicted for selected Eurasia-North America and Nubia-North America fracture zones. Flow lines for the Gibbs fracture zone are reconstructed from stage rotations determined from the Eurasia-North America (EU-NA) best-fitting rotations in table 2 of Merkouriev & DeMets (2014a) and the noise-reduced stage rotations in Supporting Information Table 2. Flow lines for the Oceanographer fracture zone are reconstructed from stage rotations determined from the Nubia-North America (NB-NA) best-fitting rotations in table 2 of Merkouriev & DeMets (2014b) and the noise-reduced stage rotations in Supporting Information Table 2.

metres at most locations and never by more than 1 km from flow lines that are reconstructed with the best-fitting stage rotations (red lines in the upper panel of Fig. 3). The less-than 1-km differences between the flow lines are smaller than the several kilometre uncertainties associated with finding the locus of palaeo-slip within a fracture zone valley. The flow-line differences are thus unlikely to be significant. Overall, the weighted root-mean-square (wrms) misfit of the flow lines to the 1377 fracture zone crossings is only 12 per cent larger for the noise-reduced rotations than for best-fitting rotations.

Reconstructions of the magnetic reversal crossings with the noise-reduced rotations increase the wrms misfit by ∼20 per cent relative to the misfit for the best-fitting rotations. The wrms misfits for 18 of the 21 rotations increased by only 0–300 m, which we consider too small to matter in plate tectonic reconstructions. Increases of 1–2 km in the wrms misfits occurred for reconstructions of reversal crossings C5n.1 (9.79 Ma), 5n.2 (11.06 Ma) and 5An.2 (12.47 Ma). All three of these reconstructions are associated with erratic variations in the interval spreading rates as determined from the best-fitting stage angular velocities (Merkouriev & DeMets 2014a). The original reversal identifications may thus be systematically mislocated by 1–2 km.

4.1.3 Interval-velocity history

The noise-reduced rotations confirm the plate kinematic history originally reported by Merkouriev & DeMets (2008, 2014a), whereby Eurasia-North America Plate motion since 20 Ma has consisted of two periods of relatively steady motion. During the most recent phase, spanning the past 7 Myr, the two plates have rotated around a stationary or slowly migrating pole centered on 63°N, 138°E (grey squares in Figs 2a and b). Before 8 Ma, the two plates rotated around a pole ∼1000 km north of the present pole at an angular rate ∼30 per cent faster than at present (Fig. 2c).

Based on the good fit of an assumed-stationary pole and fixed angular rotation rate to all the data since 6.7 Myr, Merkouriev & DeMets (2014a) suggest that plate motion during the past 6.7 Myr may have been steady. The REDBACK opening poles instead migrate smoothly southward for the past 7 Myr (Fig. 2b), representing a more complex description of the recent motion, but also illustrating the ability of REDBACK to reduce the impact of noise in a rotation sequence without sacrificing any of its inherent temporal resolution.

Fig. 4 shows interval spreading rates and directions that are predicted near the Azores Triple Junction by the newly estimated, noise-reduced Eurasia-North America stage angular velocities (Supporting Information Table 2) and stage angular velocities determined from the original best-fitting rotations of Merkouriev & DeMets (2014a). The former predict a less erratic spreading history than the latter and thus accomplish the intended effect of the Bayesian methodology. The ∼20 per cent spreading-rate slowdown at 8–6.5 Ma originally described by Merkouriev & DeMets (2008, 2014a) is clearly seen in the noise-reduced solution (Fig. 4a). The predicted, noise-reduced slip directions are remarkably well-behaved in comparison to interval directions determined from the best-fitting solution (Fig. 4b) and indicate that the direction of plate slip near the Azores Triple Junction has remained steady since at least 20 Ma. During the past 6 Myr, both the opening rate and direction near the Azores Triple Junction (and elsewhere along the plate boundary) have remained steady within the approximate ±0.5 mm yr^{-1} and ±0.5° resolutions of the predicted plate velocities.

Our REDBACK analysis also suggests that a smaller, previously unidentified change in motion may have occurred at 14–13 Ma.

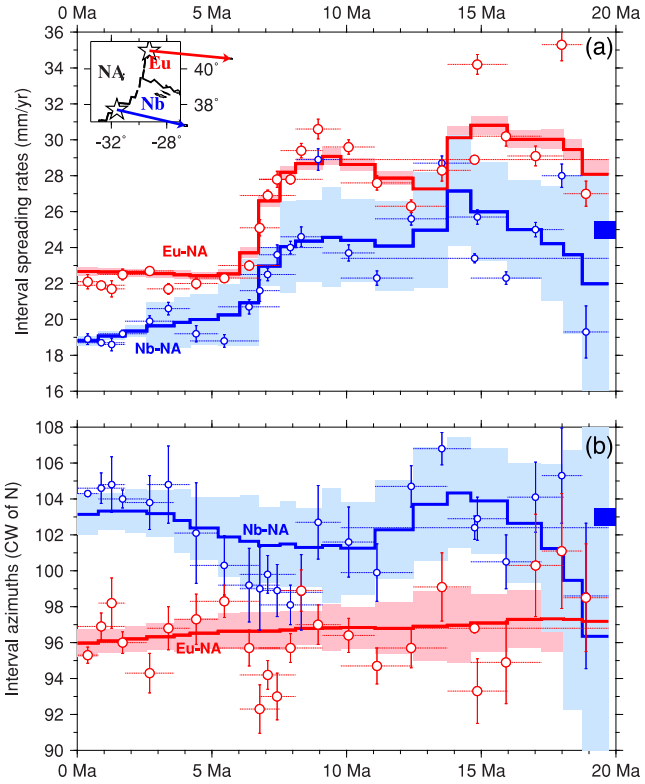

Figure 4. Nubia-North America (Nb-NA) and Eurasia-North America (Eu-NA) interval seafloor spreading rates (a) and azimuths (b) at the locations of the stars in the inset map. Circles show interval rates determined from the best-fitting rotations of Merkouriev & DeMets (2014a,b). Solid red and blue lines show predictions of the noise-reduced angular velocities in Supporting Information Tables 2 and 4. The blue boxes at the rightmost edges of (a) and (b) show the interval rate and direction that are predicted by a 25.1–19.7 Ma stage angular velocity (see text). Horizontal dotted lines show the time interval spanned by a given stage angular velocity. All rotations are corrected for outward displacement. All uncertainties are 1-σ. The inset map shows MORVEL velocity predictions at locations indicated by the stars (DeMets *et al.* 2010).

We are however less confident about this result because it depends heavily on the accuracy of Merkouriev & DeMets's identifications of the hard-to-identify, short-duration anomalies in the 5AA-5AD reversal sequence (spanning ages of 13–15 Ma).

4.2 Nubia-North America kinematics since 20 Ma

4.2.1 Best-fitting finite rotations

The finite opening poles that best reconstruct the numerous magnetic reversal and fracture zone crossings from the Nubia-North America segment of the Mid-Atlantic Ridge (from table 2 of Merkouriev & DeMets 2014b) generally cluster near 80°N, 45°E (Fig. 5a), but include outliers such as the poles for C5n.1 and C6no that are probably caused by data noise rather than a change in plate motion. The best-fitting opening angles are generally well-behaved except for anomalous best-fitting angles for C5n.1 and C6no (Fig. 5c). The larger noise in the C5n.1 and C6no angles is attributable in part to their anomalous pole locations due to the well-known trade-off between the location of a pole and the magnitude of its rotation angle.

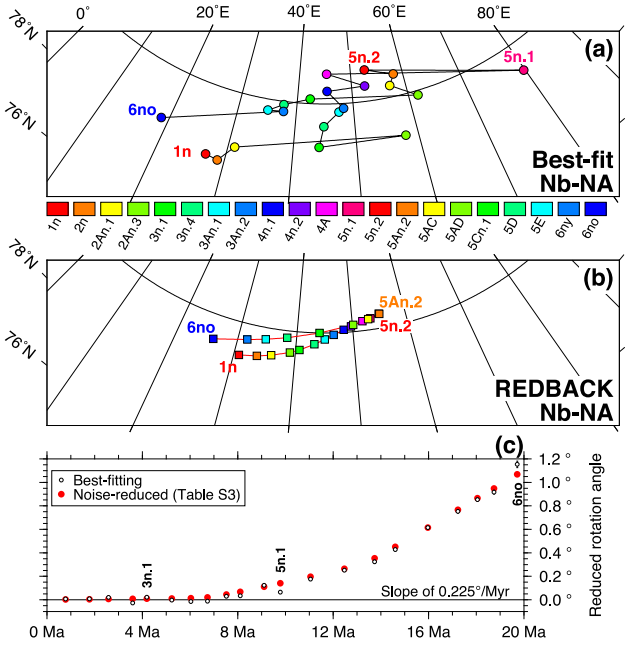

Figure 5. Comparison of Nubia-North America finite rotation poles and angles before and after noise reduction. (a) Best-fitting finite rotation poles from table 2 of Merkouriev & DeMets (2014b). (b) Noise-reduced finite rotation poles from Supporting Information Table 3. (c) Best-fitting and noise-reduced angles reduced by a slope of 0.225° Myr^{-1}.

4.2.2 Noise-reduced rotations and fits

As expected, the REDBACK analysis produces Nubia-North America finite rotations and stage angular velocities (Supporting Information Tables 3 and 4, respectively) that are less noisy than the 21 best-fitting rotations from which they were determined. The REDBACK poles migrate steadily eastward between 19.7 Ma (C6no) and 12.5 Ma (C5An.2) and then move westward (Fig. 5b). The finite opening angles from the REDBACK analysis (red circles in Fig. 5c) also evolve less erratically through time. A clear change at ~7 Ma in the rates of angular opening defined by the REDBACK and best-fitting opening-angles marks the 20 per cent spreading-rate slowdown previously described by Merkouriev & DeMets (2014b). The significance of a second, more subtle change in the angular rotation rate at ~13 Ma is discussed below.

Flow lines that we reconstructed for the Oceanographer Fracture Zone with the best-fitting and noise-reduced stage rotations (red and black lines, respectively, in the lower panel of Fig. 3) differ by only a few hundred metres in location and are both consistent with the fracture zone bathymetry. We consider these differences to be insignificant. Reconstructions of the magnetic reversal crossings with the 21 noise-reduced finite rotations increase the misfits by 300 m or less for all 21 rotations, too small to be significant in plate tectonic reconstructions. The Nubia-North America rotation sequence determined from REDBACK is therefore consistent with the original kinematic data.

4.2.3 Interval-velocity history

The noise-reduced Nubia-North America stage angular velocities predict two periods of relatively steady plate motion since 20 Ma, as originally reported by Merkouriev & DeMets (2014b). At a location near the Azores Triple Junction, seafloor opening rates have either averaged a steady 20 ± 1 mm yr^{-1} or have declined modestly (by

1 mm yr^{-1}) during the past 6.5 Myr (Fig. 4a). The predicted opening directions have rotated ∼1° clockwise since 6.5 Ma (Fig. 4b), less than the ∼5° clockwise rotation that is predicted by the best-fitting stage rotations. Models that predict steady plate motion for the past 7 Myr are permitted within the REDBACK velocity uncertainties and may in fact be preferable given that Eurasia-North America Plate motion appears to have remained steady during the past 6.5 Myr.

The new, noise-reduced stage angular velocities predict that seafloor spreading rates before 8 Ma averaged 24 ± 2 mm yr^{-1} (Fig. 4a), ∼20 per cent faster than the opening rates since 6.5 Ma. The well-defined slowdown in Nubia-North America Plate motion at ∼7 Ma coincides with the equally well-defined 8–6.5 Ma slowdown in Eurasia-North America Plate motion (Fig. 4a), suggesting that the two had a common cause. The noise-reduced stage angular velocities predict that motion before 7 Ma was relatively steady, particularly from 14 to 7 Ma (Fig. 4). Although the REDBACK stage angular velocities predict that spreading rates from 20 to 14 Ma may have accelerated gradually and directions may have rotated ∼5° clockwise, the uncertainties are large enough to include models that predict steady motion during this period.

In order to test whether the modest acceleration and ∼8° clockwise change in the slip direction from 20 to 14 Ma were real or may instead be artifacts of data noise, we estimated a 25.1–19.7 Ma stage angular velocity from Muller *et al.*'s (1999) Nubia-North America finite rotation for C8n.1 (25.1 Ma) and our noise-reduced finite rotation for C6no (Supporting Information Table 3). The 25.1–19.7 Ma Nubia-North America stage angular velocity predicts motion near the Azores Triple Junction of 25.0 mm yr^{-1} toward N103.1°E (indicated by the blue boxes in Fig. 4). This agrees with the 24 ± 2 mm yr^{-1}, N103°E ± 2° velocity that is predicted by the noise-reduced stage angular velocities for times between ∼18 and 7 Ma (shown by the blue lines in Fig. 4). We provisionally conclude that Nubia-North America Plate motion remained steady from ∼25 to ∼7 Ma. A stronger test of the steadiness or lack thereof of the plate motion before ∼15 Ma will require more closely spaced reconstructions of Nubia-North America Plate motion for times before 20 Ma (Fig. 4).

4.3 Nubia-Eurasia plate motion since 20 Ma

4.3.1 Best-fitting versus noise-reduced rotations

Nubia-Eurasia finite rotations that we determined from the noise-reduced Eurasia-North America and Nubia-North America finite rotations are found in Table 1. Standard methods for combining finite rotations and their covariances were used to determine the Nubia-Eurasia finite rotations and their uncertainties (Chang *et al.* 1990; Kirkwood *et al.* 1999). The Eurasia-North America and Nubia-North America finite rotation sequences reconstruct the same 21 magnetic reversals and thus require no interpolation prior to combining them.

Fig. 6 compares the newly estimated Nubia-Eurasia finite rotation poles and angles to poles and angles that we determined by combining the original best-fitting Eurasia-North America and

Table 1. Nubia-Eurasia noise-reduced finite rotations.

Magnetic reversal	Age (Ma)	Lat. (°N)	Long. (°E)	Ω (degrees)	Covariances					
					a	*b*	*c*	*d*	*e*	*f*
1n	0.781	17.59	−20.96	−0.096	9.6	0.3	0.2	4.9	−6.2	7.9
2n	1.778	17.71	−20.44	−0.214	13.1	−1.5	2.6	7.9	−10.3	13.4
2An.1	2.581	17.86	−20.06	−0.306	17.7	−4.1	6.1	11.9	−15.6	20.6
2An.3	3.596	18.11	−19.65	−0.414	25.4	−8.7	12.2	18.8	−25.1	33.7
3n.1	4.187	18.25	−19.48	−0.475	31.2	−12.2	17.0	23.9	−32.2	43.8
3n.4	5.235	18.47	−19.28	−0.577	42.8	−19.5	26.6	35.0	−47.7	65.7
3An.1	6.033	18.57	−19.19	−0.650	52.5	−25.8	35.1	44.6	−61.3	85.4
3An.2	6.733	18.37	−19.16	−0.714	58.4	−30.1	41.4	50.6	−70.1	99.2
4n.1	7.528	17.76	−19.17	−0.790	59.0	−31.4	45.0	50.3	−70.2	101.9
4n.2	8.108	17.18	−19.18	−0.846	59.5	−29.3	46.4	47.5	−66.0	99.9
4A	9.105	16.11	−19.17	−0.938	62.5	−22.4	46.0	42.8	−58.7	98.3
5n.1	9.786	15.29	−19.11	−0.997	72.1	−16.3	48.7	42.4	−56.3	105.5
5n.2	11.056	14.17	−19.04	−1.107	92.2	−7.1	52.6	46.3	−61.2	131.7
5An.2	12.474	13.61	−18.73	−1.241	118.3	0.3	55.6	54.3	−76.6	172.5
5AC	13.739	14.32	−18.24	−1.388	169.5	−5.0	86.2	72.4	−101.4	222.9
5AD	14.609	14.77	−17.91	−1.510	204.1	−3.0	111.3	63.0	−85.2	210.5
5Cn.1	15.974	14.92	−17.84	−1.728	206.3	−20.4	124.8	43.7	−68.6	171.7
5D	17.235	15.11	−18.03	−1.938	182.8	−38.1	122.6	37.8	−65.3	147.2
5E	18.056	15.10	−18.30	−2.078	173.8	−47.9	123.5	39.5	−68.7	143.6
6ny	18.748	15.12	−18.59	−2.198	200.2	−65.0	150.1	49.6	−85.1	170.4
6no	19.722	15.30	−19.23	−2.392	241.9	−114.6	198.2	97.0	−149.2	244.7

Notes. These finite rotations reconstruct movement of the Nubia Plate relative to the Eurasia Plate and are constructed from the Eurasia-North America and Nubia-North America finite rotations in Supporting Information Tables 1 and 3. Reversal ages are adopted from the GTS12 time scale of Ogg (2012). Rotation angles Ω are positive anticlockwise. The Cartesian rotation covariances are calculated in a Nubia-fixed reference frame and have units of 10^{-8} radians^2. Elements a, *d* and *f* are the variances of the (0°N, 0°E), (0°N, 90°E), and 90°N components of the rotation. The covariance matrices are reconstructed as follows:

$$\begin{pmatrix} a & b & c \\ b & d & e \\ c & e & f \end{pmatrix}$$

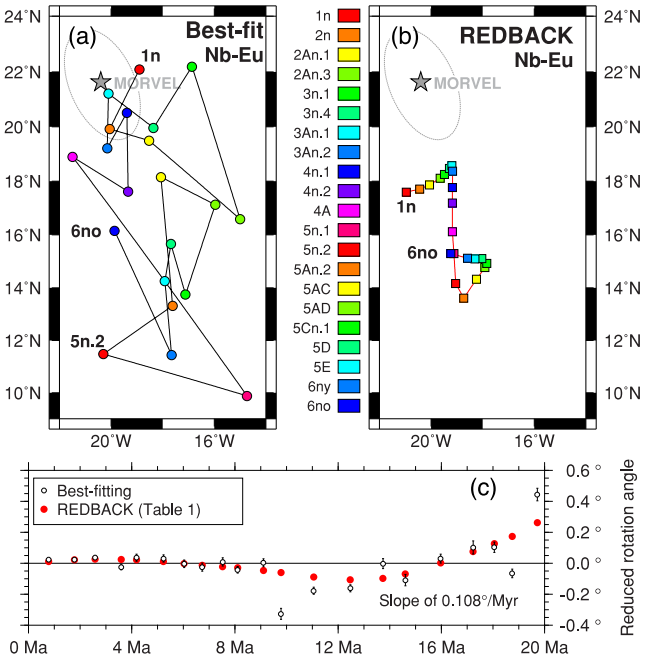

Figure 6. Comparison of Nubia-Eurasia finite rotation poles and angles determined from (a) best-fitting Eurasia-North America and Nubia-North America rotations from Merkouriev & DeMets (2014a,b) and (b) noise-reduced Eurasia-North America and Nubia-North America rotations in Supporting Information Tables 1 and 3. The Nubia-Eurasia REDBACK rotations are given in Table 1. (c) Best-fitting and noise-reduced rotation angles reduced by a slope of 0.108° Myr^{-1}. The MORVEL pole location and 2-sigma (95 per cent) confidence region are also shown in panels a and b.

Nubia-North America finite rotations of Merkouriev & DeMets (2014a,b). Whereas the best-fitting poles change erratically through time (Fig. 6a), the Nubia-Eurasia poles determined from the Eurasia-North America and Nubia-North America REDBACK rotations are more tightly clustered and describe a simpler migration path (Fig. 6b). The sequence of rotation angles also varies less erratically than for the best-fitting rotations (Fig. 6c). Our use of Bayesian inference to identify less noisy finite-rotation sequences for the Eurasia-North America and Nubia-North America plate pairs thus produces a kinematically simpler description of Nubia-Eurasia plate motion without significantly increasing the misfit to the observations that were used to estimate the best-fitting rotations.

4.3.2 *Comparison to the independently mapped Gloria Fault*

In order to evaluate the accuracy of our newly estimated rotations, we compared Nubia-Eurasia slip directions that are predicted by stage angular velocities that we determined by differentiating the Nubia-Eurasia finite rotations in Table 1 to the trace of the Gloria Fault (located by the green line in Fig. 7), a ∼400-km-long, strike-slip oceanic fault east of the Azores Islands that has been surveyed with GLORIA side-scan sonar (Laughton *et al.* 1972). Argus *et al.* (1989) conclude that present-day Nubia-Eurasia Plate motion is concentrated along this feature based on the good fit of a Nubia-Eurasia 3 Myr average angular velocity that they estimated by invoking closure of the Nubia-Eurasia-North America Plate circuit to the trace of the Gloria Fault.

Nubia-Eurasia stage angular velocities (Table 2) are located ∼1500–2000 km south of the Gloria Fault (Fig. 7). The angular velocities that describe motion during the past 2 Myr predict slip directions along the Gloria Fault that agree within ± 2° with the N85°E ± 3° fault azimuth mapped from 22.5 to 21.5°W (inset P2 of Fig. 7) and predict directions within 5° of the fault azimuth at locations west of 22.5°W. The good agreement is not however limited to the past 2 Myr—directions that are predicted by angular velocities that span all intervals during the past ∼11 Myr differ by less than ± 6° from the measured fault trace.

From the above, we conclude the following: (1) The Gloria Fault has accommodated most or all Nubia-Eurasia Plate motion along this part of the plate boundary since at least 11 Ma. (2) Our newly estimated stage angular velocities predict directions along the western end of the Nubia-Eurasia Plate boundary that are accurate to ±5°.

4.3.3 *Interval-velocity history*

Our new stage angular velocities predict that Nubia-Eurasia motion during the past ∼13 Myr has been slow and relatively steady, ranging from only 4 mm yr^{-1} near the Azores Triple Junction to 7 mm yr^{-1} in the central Mediterranean (insets P1–P4 in Fig. 7) and centred on stage poles directly south of the Gloria Fault (Fig. 7). Rates of motion since 13 Ma have varied by less than ± 2 mm yr^{-1} from the average rate since 13 Ma and variations in the slip directions are smaller than the velocity uncertainties. No obvious first-order change in Nubia-Eurasia Plate motion occurred during the well-documented slowdowns in Eurasia-North America and Nubia-North America seafloor spreading rates at 8–6.5 Ma, although a 1–2 mm yr^{-1} slowdown may have occurred (Fig. 7).

The largest change in motion since 20 Ma was an apparently significant, factor-of-two decrease in the plate rate between 20 and 13 Ma everywhere along the plate boundary (blue lines in insets P3 and P4 of Fig. 7). Our interval rotations also predict that the plate slip direction rotated slowly anticlockwise from 20 to 13 Ma; however, the change in direction is smaller than the estimated uncertainties and is thus less robust. In general, variations in the predicted interval slip directions during the past 20 Myr (red lines in insets P1-P4 in Fig. 7) are too small and/or too short-lived to permit us to conclude with any confidence that a significant change in direction has occurred since 20 Ma.

In the next section, we extend our analysis of Nubia-Eurasia plate motion back to 55 Ma to determine whether the apparent slowdown in motion and possible anticlockwise change in the slip direction from 20 to 13 Ma concluded a longer term change in motion that may have started before ∼20 Ma or whether one or both could instead be artifacts of our data or noise-reduction methodology.

5 DISCUSSION

5.1 Post-55 Ma Nubia-Eurasia convergence in the central Mediterranean

The factor-of-two slowdown in Nubia-Eurasia convergence rates from 20 to 13 Ma (Fig. 7) motivated us to examine more closely the history of convergence between Africa and Eurasia since the beginning of the Eocene (55 Ma), a period that encompasses three important, well-dated events that affected the Mediterranean region and northern portion of the Africa Plate during this time: the Messinian salinity crisis at 6.3–5.6 Ma (Rouchy & Caruso 2006), the post-30 Ma detachment of the Arabian peninsula from the Africa Plate via rifting across the Gulf of Aden and Red Sea (Bosworth *et al.* 2005), and the widespread formation of extensional basins in the Mediterranean basin at 30–25 Ma (Jolivet & Faccenna 2000).

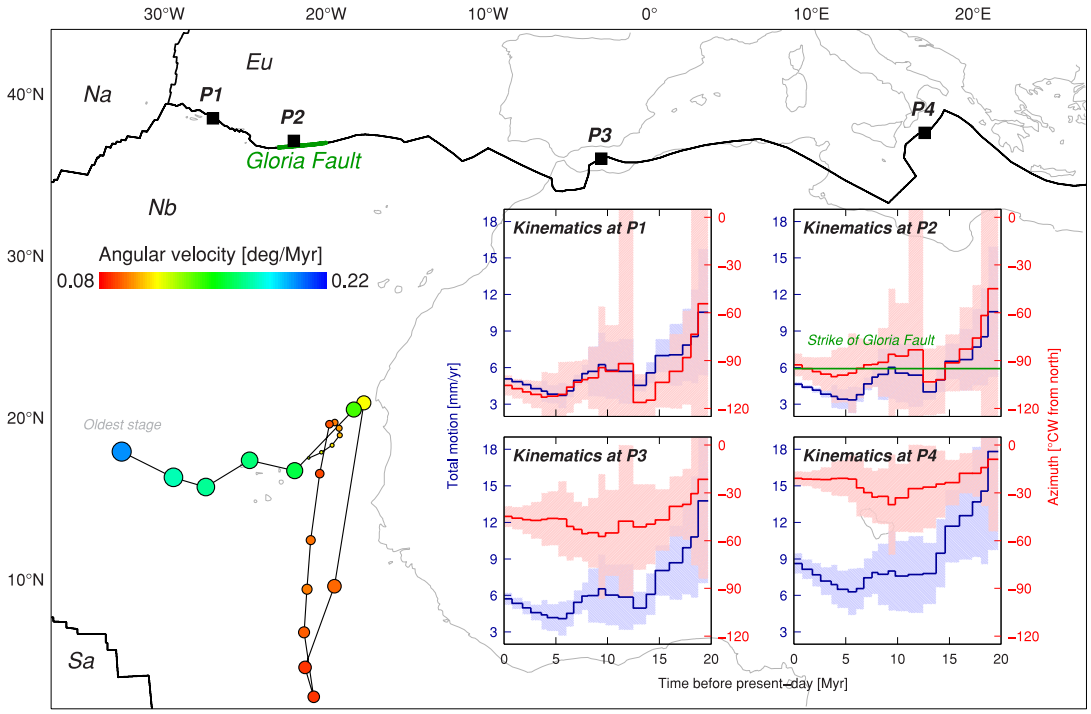

Figure 7. Nubia-Eurasia stage pole locations (circles) and their corresponding angular rotation rates (Table 2) derived from the finite rotations in Table 1. Insets show the 20 Ma to present interval rates (blue) and slip directions (red) that are predicted by the new stage angular velocities at four locations along the plate boundary. Uncertainties are 95 per cent.

Table 2. Nubia-Eurasia noise-reduced stage angular velocities.

Age(o) (Ma)	Age(y) (Ma)	Lat. (°N)	Long. (°E)	$\dot{\omega}$ (deg. Myr^{-1})	Covariances					
					a	*b*	*c*	*d*	*e*	*f*
0.781	0.000	17.59	−20.96	0.123	15.73	0.46	0.35	8.00	−10.23	13.17
1.778	0.781	17.80	−20.01	0.119	22.82	−1.27	2.90	12.89	−16.70	21.80
2.581	1.778	18.22	−19.16	0.113	47.67	−8.73	13.64	30.69	−40.46	53.72
3.596	2.581	18.80	−18.48	0.107	41.77	−12.44	17.94	29.74	−39.83	53.78
4.187	3.596	19.22	−18.33	0.102	162.10	−59.79	84.48	122.32	−165.48	226.33
5.235	4.187	19.51	−18.38	0.098	67.44	−28.78	40.10	53.67	−73.42	101.65
6.033	5.235	19.37	−18.47	0.092	149.70	−71.02	97.97	124.95	−172.79	242.01
6.733	6.033	16.28	−18.86	0.091	226.40	−114.10	157.75	194.18	−270.89	384.28
7.528	6.733	12.14	−19.19	0.097	185.75	−97.31	138.13	159.70	−224.31	324.65
8.108	7.528	9.07	−19.19	0.098	352.24	−180.48	274.63	290.77	−409.08	612.30
9.105	8.108	6.35	−19.06	0.094	122.80	−52.10	93.91	90.86	−126.76	203.48
9.786	9.105	2.33	−18.12	0.088	290.33	−83.59	206.34	183.82	−250.48	448.33
11.056	9.786	4.11	−18.34	0.088	101.90	−14.53	63.45	55.00	−73.57	150.04
12.474	11.056	9.06	−16.18	0.095	104.73	−3.40	54.33	50.06	−69.20	154.38
13.739	12.474	20.33	−14.02	0.117	179.88	−2.93	89.49	79.21	−112.33	252.12
14.609	13.739	19.81	−14.17	0.142	493.63	−10.52	263.60	178.85	−249.05	584.22
15.974	14.609	15.99	−17.37	0.160	220.27	−12.57	128.02	57.25	−83.39	209.29
17.235	15.974	16.57	−19.67	0.166	244.66	−36.81	157.17	51.23	−85.03	204.61
18.056	17.235	14.86	−21.94	0.171	528.99	−127.55	368.86	114.60	−200.73	440.14
18.748	18.056	15.42	−23.63	0.175	780.96	−235.57	577.29	185.96	−324.37	668.96
19.722	18.748	16.97	−26.62	0.201	466.02	−189.22	370.91	154.52	−249.44	446.41

Notes. These angular velocities specify Nubia Plate motion relative to the Eurasia Plate during the time period given in the first two columns, as determined from the REDBACK noise-reduction software (Iaffaldano *et al.* 2014). The angular rotation rates $\dot{\omega}$ are positive anticlockwise for the old to the young limit of each time interval. The Cartesian angular velocity covariances are calculated in a Nubia-fixed reference frame and have units of 10^{-8} radians^2 Myr^{-2}. The footnotes for Table 1 provide further information about the covariances.

5.1.1 Additional rotations from published sources

We extended estimates of (Nubia,Africa)-Eurasia Plate motion back to 55 Ma using Nubia/Africa-Eurasia rotations from two sources. Rosenbaum *et al.* (2002) estimate Africa-Eurasia finite rotations at 5 Myr intervals by interpolating pre-existing Africa-North America and Eurasia-North America finite rotations for magnetic reversals C5 (11 Ma), C6 (19 Ma), C13 (33 Ma), C21 (46 Ma) and C24 (53 Ma). From their 5-Myr-interpolated finite rotations, we determined stage rotations and hence stage angular velocities that describe Nubia-Eurasia plate motion at 5 Myr intervals from 55 Ma to the present. These interpolated stage rotations capture the first-order characteristics of Nubia-Eurasia motion since 55 Ma, but cannot be used as a reliable means of dating any changes in motion because of the irregular, wide spacing between the finite rotations from which they are derived.

We also determined stage rotations from Nubia-Eurasia finite rotations that are estimated by Vissers & Meijer (2012) from their compilation of pre-existing Africa-North America and Eurasia-North America rotations for C6(y) (18.75 Ma), C13(y) (33.16 Ma), C18n.1(o) (39.63 Ma), C21(middle) (46.54 Ma) and C24(middle) (53.38 Ma). The Nubia-Eurasia rotations estimated by Vissers & Meijer (2012) include adjustments to Eurasia-North America rotations to compensate for the pre-35 Ma motion of the Porcupine plate relative to Eurasia. Only a few of the Eurasia-North America and Africa-North America rotations that were selected by Rosenbaum *et al.* (2002) and Vissers & Meijer (2012) to estimate their Africa-Eurasia rotations come from common sources. The two sets of Africa-Eurasia rotations are thus largely, but not completely independent.

Where relevant, we used magnetic reversal age estimates from GPTS12 (Ogg 2012) to calculate interval displacement rates from the stage rotations that we derived from the finite rotations described above. Differences between the reversal ages used by the original authors and the revised ages used herein were generally too small to affect the results or conclusions presented below.

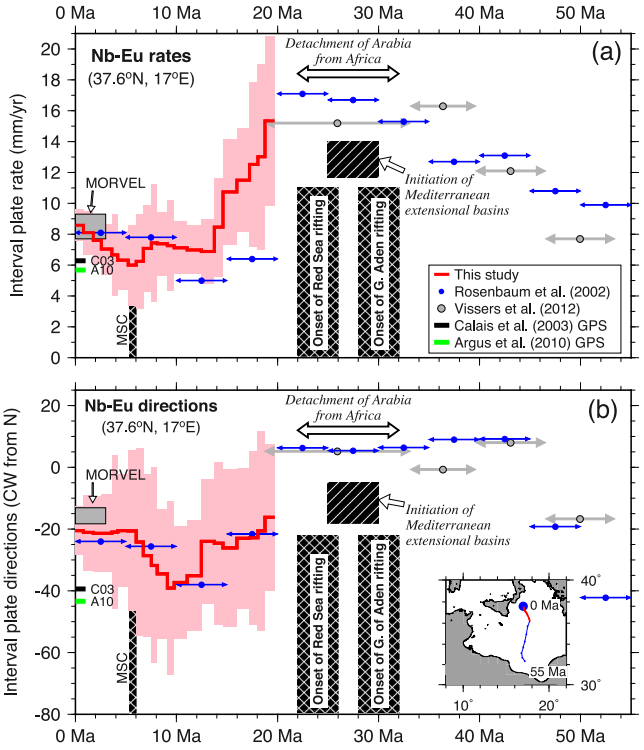

Figure 8. Nubia relative to Eurasia interval velocities, 55 Ma to present, at 37.6°N, 17.0°E (location shown in inset) predicted by stage angular velocities in Table 2 and sources listed in the legend and cited in the text. (a) Predicted interval rates with their 95 per cent uncertainties (pink shaded area), if available. GPS velocity estimates are aligned along the left-hand axis. Horizontal bars indicate the time interval spanned by each stage angular velocity. (b) Predicted interval directions with their 95 per cent uncertainties, if available. Inset shows the path of a point on the Nubia plate, reconstructed back in time relative to Eurasia, using finite rotations from Table 1 for the present to 19.7 Ma (red path) and from Rosenbaum *et al.* (2002) for 25 to 55 Ma (blue path). A10, Argus *et al.* (2010); C03, Calais *et al.* (2003); MSC, Messinian Salinity Crisis.

5.1.2 55-Ma-to-present interval velocity history

Fig. 8 shows interval velocities in the central Mediterranean since 55 Ma as predicted by our stage angular velocities (red lines in Fig. 8) and by the stage angular velocities that we determined from the Rosenbaum *et al.* (2002) and Vissers & Meijer (2012) finite rotations. Convergence rates that are predicted by the latter two sets of stage angular velocities increase from ∼8–10 mm yr^{-1} at ∼50 Ma to 16–17 mm yr^{-1} from 35 to 20 Ma (grey and blue lines in Fig. 8a). The same angular velocities predict that the convergence direction rotated 30–50° clockwise between 55 and 35 Ma (Fig. 8b). The lack of finite rotations intermediate in age between Chron 13 (33 Ma) and Chron 6 (20 Ma) precludes more detailed estimates of stage velocities from 33 to 20 Ma.

The interval velocities that are predicted by our newly estimated stage angular velocities and the stage rotations we determined from Rosenbaum *et al.*'s (2002) rotations for Chrons 6 (19.7 Ma) and 5 (11 Ma) agree well despite the order-of-magnitude difference in their temporal resolutions. For example, our 19.7 to 18.8 Ma stage angular velocity predicts a convergence rate of 15.3 mm yr^{-1}, nearly the same as the 16–17 mm yr^{-1} rate that is predicted for the preceding 15-Myr period (35–20 Ma). Our stage angular velocities predict that Nubia-Eurasia Plate motion decreased by ∼50 per cent from 15 mm yr^{-1} at 20–18 Ma to 7–8 mm yr^{-1} for the past 13 Myr (Fig. 8), consistent with the roughly factor-of-two slowdown predicted by the stage angular velocities we determined from the Rosenbaum *et al.* (2002) rotations.

The interval directions predicted by our new angular velocities and those determined from the Rosenbaum *et al.* (2002) rotations also agree to within ± 5° for the past 20 Myr (blue and red lines in Fig. 8b), lending confidence in both estimates. Interestingly, for the period 30–20 Ma, the predicted N08°E interval direction is ∼30° clockwise from the interval direction that has predominated for the past 20 Ma. A significant anticlockwise rotation of the convergence direction in the central Mediterranean thus appears to have occurred in the past 20–30 Myr.

We interpret the consistency of these independently-derived interval-velocity histories as evidence that the kinematic changes predicted by our stage angular velocities for 20–13 Ma are real rather than artifacts of our observations or noise-reduction methodology. Unfortunately, we cannot determine precisely when the convergence slowdown and anticlockwise rotation of the slip direction began because the next oldest reconstruction before Chron 6 is for Chron 13 (33 Ma). Strictly interpreted, the available rotations preclude an onset date later than 19.7 Ma for the change in motion, but permit an onset date that is millions of years earlier. Geological evidence that extensional basins formed throughout the Mediterranean region from 30 to 25 Ma, possibly in response to a slowdown in

Africa-Eurasia convergence rates (Jolivet & Faccenna 2000), indirectly favors an onset date millions of years earlier than 19.7 Ma.

GPS measurements further confirm the slowdown and anticlockwise rotation of Nubia-Eurasia plate motion since 20 Ma. For example, Nubia-Eurasia angular velocities derived by Calais *et al.* (2003) and Argus *et al.* (2010) from geodetic velocities predict respective velocities of 5.7 mm yr^{-1}, N39.4°W and 6.3 mm yr^{-1}, N43.4°W in the central Mediterranean (labelled 'C03' and 'A10' in Fig. 8). Both are slower than and anticlockwise from the motion that is predicted for times before 20 Ma.

5.1.3 Implications for Arabia Plate detachment and the Messinian Salinity Crisis

One possible cause of the Neogene (or earlier) change in Nubia-Eurasia motion described above may have been the Oligocene-to-early-Miocene breakup of the Afro-Arabia plate, during which the then-northward-subducting Arabia Peninsula detached from the larger, more slowly moving Africa Plate via opening across the Gulf of Aden and Red Sea (e.g. Bosworth *et al.* 2005). The detachment of the more-rapidly moving Arabia Plate from Africa presumably reduced the northward-directed component of slab pull that was driving Africa's northward convergence with Eurasia. By implication, convergence between Nubia and Eurasia would have slowed down.

Volcanic activity and faulting associated with the detachment of Arabia from Africa began synchronously at 24 ± 2 Ma everywhere along the length of the present Red Sea, which defines the present-day Arabia-Nubia Plate boundary (Bosworth *et al.* 2005). Continental rifting in the Gulf of Aden, marking the birth of the Arabia-Somalia Plate boundary, began several million years earlier (Bosworth *et al.* 2005). The detachment of Arabia from the larger Africa Plate was thus complete by 24 ± 2 Ma. A strong test of whether the decline in Nubia-Eurasia convergence rates preceded, followed, or coincided with the Arabia Plate detachment awaits future, more closely spaced reconstructions of Atlantic basin magnetic reversals between existing reconstructions for Chron 6 (19.7 Ma) and Chron 13 (33 Ma) (Rosenbaum *et al.* 2002; Vissers & Meijer 2012).

No significant change in Nubia-Eurasia Plate motion occurred immediately before or during the well-dated Messinian salinity crisis (Fig. 8), during which kilometre-scale fluctuations in the Mediterranean Sea level caused the deposition of deep marine evaporites at 6.3–5.6 Ma and dessication of much of the Mediterranean Basin (Rouchy & Caruso 2006). Although the long-term narrowing of the Mediterranean basin due to convergence between Nubia and Eurasia undoubtedly set the stage for the salinity crisis, as concluded by Jolivet *et al.* (2006), our results argue strongly against the possibility that a major change in plate motion such as a sudden speedup in the convergence rate may have triggered or contributed to the salinity crisis.

5.2 Discrepancy with GPS estimates

Calais *et al.* (2003) report that a Nubia-Eurasia angular velocity that best fits the velocities of 18 continuous GPS sites on the two plates is located ~3000 km south of an angular velocity that best fits 500 3.16-Myr-average seafloor spreading rates and nine transform fault azimuths from the Nubia-Eurasia-North America plate circuit. Here, we update that comparison using our newly estimated stage poles (Table 2) and including more recent geodetic estimates of Nubia-Eurasia Plate motion (Fig. 9a).

Nubia-Eurasia poles determined from geodetic observations are generally located south of the Gloria Fault (Fig. 9a) and fall within the 95 per cent confidence region of the geodetic pole estimated by Argus *et al.* (2010), which is located near the center of the geodetic estimates (Fig. 9a). Our newly estimated geologic stage poles are located ~3000 km north of the geodetic poles, far outside the 95 per cent confidence region of the Argus *et al.* pole. The discrepancy between our new geologic poles and all previously published geodetic estimates is thus as large as found by Calais *et al.* (2003). Our new stage poles are however located close to the 3.16-Myr-average MORVEL Nubia-Eurasia pole (DeMets *et al.* 2010 and Fig. 9a) and predict velocities similar to those predicted by

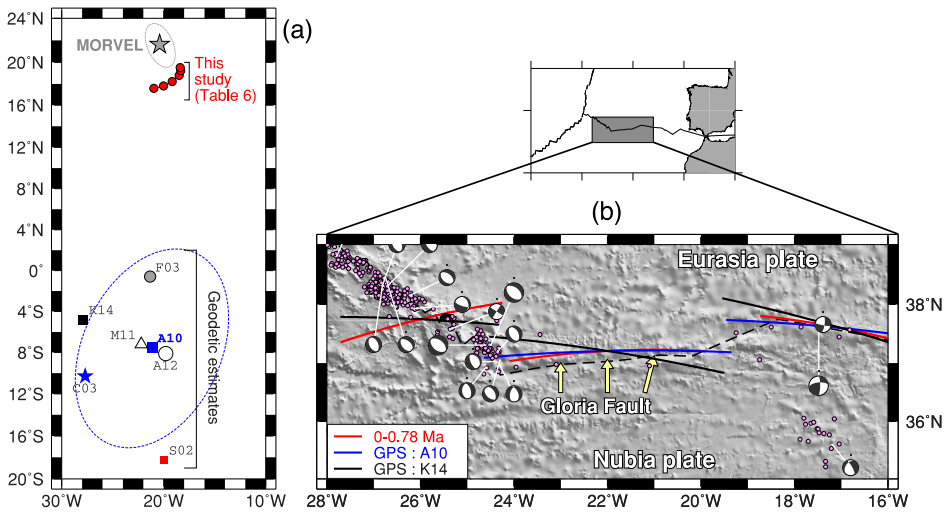

Figure 9. (a) Estimates of geologically recent Nubia-Eurasia poles as follows: red circles indicate stage poles from Table 2 for 5.2 Ma to the present; grey star shows the 3.16 Myr average MORVEL estimate (DeMets *et al.* 2010); S02, Sella *et al.* (2002) GPS estimate; C03, Calais *et al.* (2003) GPS estimate; F03, Fernandes *et al.* (2003) GPS estimate; A10, Argus *et al.* (2010) geodetic estimate; A12, Altamimi *et al.* (2012) geodetic estimate; K14, Kreemer *et al.* (2014) GPS estimate. The dotted blue line shows the 2-D 95 per cent confidence ellipse for the Argus *et al.* (2010) pole. (b) Kinematic map centred on the Gloria strike-slip fault. Map shows seafloor bathymetry, 1963–2014 earthquakes, and 1976–2014 Global centroid moment tensor solutions (Ekstrom *et al.* 2012). The dashed black line shows the plate boundary as interpreted from bathymetry, GLORIA (Laughton *et al.* 1972), and earthquakes. Bathymetry is overlain by small circles around the pole given in Table 2 for the past 0.78 Ma (red line), and two recently estimated geodetic poles shown in Panel a (blue and black small circles). The predicted small circles are offset ~20 km north of the Gloria Fault for clarity and thus should parallel, but not overlay the trace of the fault.

the MORVEL angular velocity (Fig. 8). The two geologic estimates are thus highly consistent.

The large difference between the geologic and geodetic estimates is puzzling. Although Calais *et al.* (2003) suggest that the difference could indicate that Nubia-Eurasia Plate motion has changed since 3 Ma, our new stage rotations for times since 5 Ma have instead remained relatively stationary (Fig. 9a) and predict relatively steady interval velocities (Fig. 8). Our newly estimated rotations thus reveal no obvious change in plate motion since 5 Ma that might reconcile the large discrepancy between the geologic and geodetic estimates.

As a test, we used the well-mapped trace of the Gloria Fault as an independent means of evaluating the accuracy of our Nubia-Eurasia stage poles and recently published geodetic poles. Assuming that the Gloria Fault accommodates strike-slip motion between Nubia and Eurasia, poles that accurately describe Nubia-Eurasia motion should predict small circles that match the trace of the Gloria Fault (Fig. 9b). A small circle around our youngest stage pole (0–0.78 Ma) closely parallels the fault trace (compare red and dashed black lines in (Fig. 9b). More generally, all of the stage rotations for intervals back to 11 Ma predict directions that agree with the fault trend within several degrees (see inset for location P2 in Fig. 7).

All but two of the geodetic estimates of Nubia-Eurasia plate motion are also consistent with the hypothesis that the Gloria Fault is a narrow, strike-slip boundary separating the two plates. A small circle that is centred on the geodetic pole of Argus *et al.* (2010) fits the fault trace well (blue line in Fig. 9b), as do other geodetic estimates with poles that are close to that estimated by Argus *et al.* Two of the seven geodetic estimates, those of Kreemer *et al.* (2014) (black line in Fig. 9b) and Calais *et al.* (2003) (not shown), misfit the trace of the Gloria Fault and are thus unlikely to describe accurately present-day Nubia-Eurasia Plate motion.

Systematic biases may affect one or both of the geodetic and/or geologic estimates. Merkouriev & DeMets (2008) describe large differences between their high-resolution determinations of Eurasia-North America rotation poles and geodetic estimates (see their Fig. 17), whereby some of the geodetically derived poles that were then available were located up to ∼1000 km north of the geologic poles. More recent geodetic estimates of Eurasia-North America pole locations (Argus *et al.* 2010; Altamimi *et al.* 2012) have exacerbated rather than diminished these differences. Some geodetic poles are located so far north in the Arctic Basin that they predict convergent motion across parts of the Arctic Basin seafloor spreading system, where ridge-normal extension instead dominates (Altamimi *et al.* 2007, 2012).

The implausibility of some of the geodetic solutions and persistent northward bias of all geodetic solutions for Eurasia-North America motion relative to the geologic solutions suggests that geodetic estimates of Eurasia Plate motion may all be affected to varying degrees by a common, poorly understood systematic bias, possibly due to slow distributed deformation or unmodelled glacial isostatic rebound within the Eurasia plate. By implication, geodetic estimates of Nubia-Eurasia Plate motion may be biased.

Alternatively, Eurasia-North America rotations determined from marine magnetic reversals and fracture zones may be systematically biased. If so, the high degree of consistency of the rotations that describe motion during the past 5 Myr (Fig. 4 and Tables 1 and 2) requires that any such bias affects reconstructions for multiple independent times. Biases that span multiple reconstructions might arise from systematic misidentifications of young magnetic reversals along some part of the Eurasia-North America Plate boundary, possibly in the Arctic basin, where ultra-slow spreading rates create a low-fidelity magnetic anomaly sequence. Alternatively, unrecognized deformation in the past few Myr within the Eurasia or North America plates might bias our rotation estimates.

Finally, we cannot exclude the possibility that Nubia-Eurasia motion has changed significantly in the past few hundred thousand years, a time period beneath the resolution of our geologic stage rotations. If so, this implies that motion has decreased 25 per cent and rotated 20° anticlockwise within the past few hundred thousand years (Fig. 8). This explanation is unappealing because it implies a more complex (and possibly untestable) kinematic model than is warranted by the already numerous data and because such a rapid change in plate motion may imply implausibly rapid changes in the torques that are acting on one or both plates.

Absent any satisfying explanation for the discrepancies that are described above, their cause remains a topic for future work.

6 CONCLUSIONS

Motion between the Nubia and Eurasia plates for much of the past 20 Myr has been slower than 10 mm yr^{-1}, posing challenges to efforts to reconstruct their relative motion with high precision. We apply trans-dimensional, hierarchical Bayesian inference to newly available rotations that reconstruct Eurasia-North America and Nubia-North America plate motions at ∼1 Myr intervals since 20 Ma to reduce noise and better estimate the motions between the three plates. Upon noise reduction, the Eurasia-North America and Nubia-North America kinematic histories during the Neogene and Quaternary are less erratic than previously inferred and do not significantly degrade the fits to the numerous magnetic reversal and fracture zone crossings that were used to estimate their noisier, best-fitting rotations. In accord with previous work, Eurasia-North America seafloor spreading rates varied modestly from 20 to ∼8 Ma, slowed down by ∼20 per cent around 7 Ma, and have remained remarkably steady since then. Eurasia-North America spreading directions appear to have remained unchanged since 20 Ma. Nubia-North America spreading rates also slowed down by ∼20 per cent around 7 Ma, and to first order have changed little since then, as previously reported.

Nubia-Eurasia finite and stage rotations estimated by closing the Nubia-North America-Eurasia plate circuit predict that convergence in the Mediterranean region slowed down by a factor of two between 20 Ma (or possibly earlier) and 13 Ma, but has remained steady or increased modestly since ∼7 Ma. The new rotations predict that slip directions along the plate boundary have remained locally parallel to the well-mapped, strike-slip Gloria Fault west of Gibraltar since ∼11 Ma and in general have varied by less than ∼10° since ∼11 Ma. Over longer time scales, our new rotations and lower resolution rotations based on previously published work predict that a factor-of-two slowdown and ∼30° anticlockwise rotation of Nubia-Eurasia motion occurred in the central Mediterranean began by 20 Ma or earlier and continued until 13 Ma, possibly in response to the 30–24 Ma detachment of the then-subducting Arabia Peninsula from the larger Africa plate. Higher-resolution reconstructions for times before 20 Ma are required to test this hypothesis. Finally, Nubia-Eurasia angular velocities estimated from geodetic and geologic observations differ significantly. Whether the source of the difference is a bias in the geodetic or geologic estimates (or both) is unclear and requires further investigation.

ACKNOWLEDGEMENTS

We thank two anonymous reviewers and the associate editor Duncan Agnew for constructive reviews. This work was supported by grants

OCE-0926274 and OCE-1433323 from the U.S. National Science Foundation. G.I. acknowledges support from the Ringwood Fellowship at the Australian National University. Most of the figures were drafted using Generic Mapping Tools software (Wessel & Smith 1991).

REFERENCES

Altamimi, Z., Collilieux, X., Legrand, J., Garayt, B. & Boucher, C., 2007. ITRF2005: a new release of the International Terrestrial Reference based on time series of station positions and Earth orientation parameters, *J. geophys. Res.,* **112,** B09401, doi:10.10292007JB004949.

Altamimi, Z., Metivier, L. & Collilieux, X., 2012. ITRF2008 plate motion model, *J. geophys. Res.,* **117,** B07402, doi:10.1029/2011JB008930.

Argus, D.F., Gordon, R.G., DeMets, C. & Stein, S., 1989. Closure of the Africa-Eurasia-North America plate motion circuit and tectonics of the Gloria fault, *J. geophys. Res.,* **94,** 5585–5602.

Argus, D.F., Gordon, R.G., Heflin, M.B., Ma, C., Eanes, R., Willis, P., Peltier, W.R. & Owen, S.E., 2010. The angular velocities of the plates and the velocity of Earth's centre from space geodesy, *Geophys. J. Int.,* **180**(3), 913–960.

ArRajehi, A. *et al.*, 2010. Geodetic constraints on present-day motion of the Arabian Plate: implications for Red Sea and Gulf of Aden rifting, *Tectonics,* **29,** TC3011, doi:10.1029/2009TC002482.

Bosworth, W., Huchon, P. & McClay, K., 2005. The Red Sea and Gulf of Aden Basins, *J. Afr. Earth Sci.,* **43,** 334–378.

Calais, E., DeMets, C. & Nocquet, J.-M., 2003. Evidence for a post-3.16 Ma change in Nubia-Eurasia-North America plate, *Earth planet. Sci. Lett.,* **216,** 81–92.

Cande, S.C. & Kent, D.V., 1995. Revised calibration of the geomagnetic polarity timescale for the Late Cretaceous and Cenozoic, *J. geophys. Res.,* **100,** 6093–6095.

Carbotte, S.M. *et al.*, 2004. New integrated data management system for Ridge2000 and MARGINS research, *EOS, Trans. Am. geophys. Un.,* **85,** 553–559.

Chang, T., Stock, J. & Molnar, P., 1990. The rotation group in plate tectonics and the representation of uncertainties of plate reconstructions, *Geophys. J. Int.,* **101,** 649–661.

DeMets, C., Gordon, R.G. & Argus, D.F., 2010. Geologically current plate motions, *Geophys. J. Int.,* **181,** 1–80.

Dewey, J.F., Helman, M.L., Turco, E., Hutton, D.H.W. & Knott, S.D., 1989. Tectonic evolution of the India/Eurasia collision zone Kinematics of the western Mediterranean, in *Alpine Tectonics,* pp. 265–283, eds Coward, M.P., Dietrich, D. & Park, R.G., Spec. Pub., Geological Society of London.

Ekstrom, G., Nettles, M. & Dziewonski, A.M., 2012. The global CMT project 2004–2010: centroid-moment tensors for 13,017 earthquakes, *Phys. Earth planet. Int.,* **200–201,** 1–9.

Fernandes, R.M.S., Ambrosius, B.A.C., Noomen, R., Bastos, L., Wortel, M.J.R., Spakman, W. & Govers, R., 2003. The relative motion between Africa and Eurasia as derived from ITRF2000 and GPS data, *Geophys. Res. Lett.,* **30,** doi:10.1029/2003GL017089.

Iaffaldano, G., Bodin, T. & Sambridge, M., 2012. Reconstructing plate-motion changes in the presence of finite-rotations noise, *Nature Commun.,* **3**, 1048, doi:10.1038/ncomms2051.

Iaffaldano, G., Bodin, T. & Sambridge, M., 2013. Slow-downs and speed-ups of India-Eurasia convergence since 20 Ma: data-noise, uncertainties and dynamic implications, *Earth planet Sci. Lett.,* **367,** 146–156.

Iaffaldano, G., Hawkins, R., Bodin, T. & Sambridge, M., 2014. REDBACK: open-source software for efficient noise-reduction in plate kinematic reconstructions, *Geochm. Geophys. Geosys.,* **15,** 1663–1670.

Ivanovic, R.F., Valdes, P.J., Flecker, R. & Gutjahr, M., 2014. Modeling global-scale climate impacts of the late Miocene Messinian Salinity Crisis, *Clim. Past,* **10,** 607–622.

Jolivet, L. & Faccenna, C., 2000. Mediterranean extension and the Africa-Eurasia collision, *Tectonics,* **19,** 1095–1106.

Jolivet, L., Augier, R., Robin, C., Suc, J.-P. & Rouchy, J.M., 2006. Lithospheric-scale geodynamic context of the Messinian salinity crisis, *Sed. Geology,* **188–189,** 9–33.

Kirkwood, B.H., Royer, J.-Y., Chang, T.C. & Gordon, R.G., 1999. Statistical tools for estimating and combining finite rotations and their uncertainties, *Geophys. J. Int.,* **137,** 408–428.

Kreemer, C., Blewitt, G. & Klein, E.C., 2014. A geodetic plate motion and Global Strain Rate Model, *Geochem. Geophys. Geosys.,* **15,** 3849–3889.

Laughton, A.S., Whitmarsh, R.B., Rusby, J.S.M., Somers, M.L., Revie, J., McCartney, B.S. & Nafe, J.E., 1972. A continuous east-west fault of the Azores-Gibraltar Ridge, *Nature,* **327,** 217–220.

Mazzoli, S. & Helman, M., 1994. Neogene patterns of relative plate motion for Africa-Europe: some implications for recent central Mediterranean tectonics, *Geol. Rundsch.,* **83,** 464–468.

McQuarrie, N., Stock, J.M., Verdel, C. & Wernicke, B.P., 2003. Cenozoic evolution of Neotethys and implications for the causes of plate motions, *Geophys. Res. Lett.,* **30**(20), 2036, doi:10.1029/2003GL017992.

Merkouriev, S. & DeMets, C., 2008. A high-resolution model for Eurasia-North America plate kinematics since 20 Ma, *Geophys. J. Int.,* **173,** 1064–1083.

Merkouriev, S. & DeMets, C., 2014a. High-resolution Quaternary and Neogene reconstructions of Eurasia-North America plate motion, *Geophys. J. Int.,* **198,** 366–384.

Merkouriev, S. & DeMets, C., 2014b. High-resolution estimates of Nubia-North America plate motion: 20 Ma to present, *Geophys. J. Int.,* **196,** 1281–1298.

Muller, R.D., Royer, J.-Y., Cande, S.C., Roest, W.R. & Maschenkov, S., 1999. New constraints on the Late Cretaceous/Tertiary plate tectonic evolution of the Caribbean, in *Caribbean Basins: Sedimentary Basins of the World*, Vol. 4, pp. 33–59, ed. Mann, P., Elsevier Science B.V., Amsterdam.

Ogg, J.G., 2012. Geomagnetic polarity time scale, in *The Geologic Time Scale 2012,* pp. 85–113, eds Gradstein, F.M., Ogg, J.G., Schmitz, M. & Ogg, G., Elsevier.

Reilinger, R. & McClusky, S., 2011. Nubia-Arabia-Eurasia plate motions and the dynamics of Mediterranean and Middle East tectonics, *Geophys. J. Int.,* **186,** 971–979.

Rosenbaum, G., Lister, G.S. & Duboz, C., 2002. Relative motions of Africa, Iberia, and Europe during the Alpine orogeny, *Tectonophys.,* **359,** 117–129.

Rouchy, J.M. & Caruso, A., 2006. The Messinian salinity crisis in the Mediterranean basin: a reassessment of the data and an integrated scenario, *Sed. Geol.,* **188–189,** 35–67.

Sella, G.F., Dixon, T.H. & Mao, A., 2002. REVEL: a model for recent plate velocities from space geodesy, *J. geophys. Res.,* **107**(B4), 2081, doi:10.1029/2000JB000033.

Vissers, R.L.M. & Meijer, P.T., 2012. Iberian plate kinematics and Alpine collision in the Pyrenees, *Earth-Sci. Rev.,* **114,** 61–83.

Wessel, P. & Smith, W.H.F., 1991. Free software helps map and display data, *EOS, Trans. Am. geophys. Un.,* **72,** 441–446.

SUPPORTING INFORMATION

Additional Supporting Information may be found in the online version of this paper:

Table S1. Eurasia-North America noise-reduced finite rotations.
Table S2. Eurasia-North America noise-reduced stage angular velocities.
Table S3. Nubia-North America noise-reduced finite rotations.
Table S4. Nubia-North America noise-reduced stage angular velocities (http://gji.oxfordjournals.org/lookup/suppl/doi:10.1093/gji/ggv277/-/DC1).

Please note: Oxford University Press is not responsible for the content or functionality of any supporting materials supplied by the authors. Any queries (other than missing material) should be directed to the corresponding author for the paper.